

# GRACE Hydrological estimates for small basins: Evaluating processing approaches on the High Plains Aquifer, USA

Laurent Longuevergne,<sup>1,2</sup> Bridget R. Scanlon,<sup>1</sup> and Clark R. Wilson<sup>2</sup>

Received 27 August 2009; revised 8 March 2010; accepted 25 March 2010; published 11 November 2010.

[1] The Gravity Recovery and Climate Experiment (GRACE) satellites provide observations of water storage variation at regional scales. However, when focusing on a region of interest, limited spatial resolution and noise contamination can cause estimation bias and spatial leakage, problems that are exacerbated as the region of interest approaches the GRACE resolution limit of a few hundred km. Reliable estimates of water storage variations in small basins require compromises between competing needs for noise suppression and spatial resolution. The objective of this study was to quantitatively investigate processing methods and their impacts on bias, leakage, GRACE noise reduction, and estimated total error, allowing solution of the trade-offs. Among the methods tested is a recently developed concentration algorithm called spatio-spectral localization, which optimizes the basin shape description, taking into account limited spatial resolution. This method is particularly suited to retrieval of basin-scale water storage variations and is effective for small basins. To increase confidence in derived methods, water storage variations were calculated for both CSR (Center for Space Research) and GRGS (Groupe de Recherche de Géodésie Spatiale) GRACE products, which employ different processing strategies. The processing techniques were tested on the intensively monitored High Plains Aquifer (450,000 km<sup>2</sup> area), where application of the appropriate optimal processing method allowed retrieval of water storage variations over a portion of the aquifer as small as ~200,000 km<sup>2</sup>.

**Citation:** Longuevergne, L., B. R. Scanlon, and C. R. Wilson (2010), GRACE Hydrological estimates for small basins: Evaluating processing approaches on the High Plains Aquifer, USA, *Water Resour. Res.*, 46, W11517, doi:10.1029/2009WR008564.

## 1. Introduction

[2] The Gravity Recovery and Climate Experiment (GRACE) satellite mission, launched in March 2002 [Tapley *et al.*, 2004], has proven to be an excellent complement to ground-based hydrologic measurements to monitor water mass storage variations within the Earth's fluid envelopes. The dominant GRACE signal reflects changes in vertically integrated stored water, including variations from snow pack, glaciated areas, surface water, soil moisture, and groundwater at all depths. In this way, GRACE data are distinctly different from those of other remote sensing satellites, which are typically limited to observations near the land surface. Extracting water storage variations of any single component (e.g., groundwater) requires disaggregating the vertically integrated water storage signal, either by making assumptions (e.g., neglecting snow or surface water contributions) or by using models or other observations to estimate certain components, such as soil moisture.

[3] Numerous studies have shown that GRACE-derived stored water variations compare favorably with ground-based measurements and hydrological models at spatial

scales of several hundred kilometers and greater. As reviewed by Ramillien *et al.* [2008], these studies provide confidence that GRACE can be used to monitor hydrological systems and to improve hydrological modeling [Lettenmaier and Famiglietti, 2006; Güntner, 2008]. GRACE data have been applied to monitoring soil moisture and/or groundwater depletion from drought or irrigation [Leblanc *et al.*, 2009; Rodell *et al.*, 2009; Tiwari *et al.*, 2009] and to extract flux information from the water balance equation, such as evapotranspiration [Rodell *et al.*, 2004b; Ramillien *et al.*, 2006] or river discharge [Syed *et al.*, 2009]. GRACE data have also been integrated into the modeling process, such as for validating global land-surface models [Ngo-Duc *et al.*, 2007], validating parameterization of land-surface schemes [Niu and Yang, 2006; Han *et al.*, 2009], and validating modifications of land-surface models (G. Y. Niu, *et al.*, The community Noah land surface model with multi-physics options, submitted to *Journal of Geophysical Research*, 2009a; G. Y. Niu *et al.*, The community Noah land surface model with multi-physics options 2. Tests over global river basins, submitted to *Journal of Geophysical Research*, 2009b). Finally, GRACE data have led to improved descriptions of water fluxes via joint calibration of hydrologic models and river discharge [Werth *et al.*, 2009] or via assimilation into land-surface models [Zaitchik *et al.*, 2008]. Such applications of GRACE data require both robust and bias-free estimates of water storage change and error estimates to appropriately weight the data [Güntner, 2008]. At the same time, interest

<sup>1</sup>Bureau of Economic Geology, Jackson School of Geosciences, University of Texas at Austin, Austin, Texas, USA.

<sup>2</sup>Department of Geological Sciences, Jackson School of Geosciences, University of Texas at Austin, Austin, Texas, USA.

in using GRACE data is expanding to smaller basins (i.e. basin areas  $\leq 250,000 \text{ km}^2$ ) and improved data processing is required to reliably estimate water storage variations at these smaller spatial scales.

[4] The GRACE mission consists of two satellites at an altitude of  $\sim 450 \text{ km}$  in an identical polar orbit, one trailing the other by  $\sim 200 \text{ km}$  [Schmidt *et al.*, 2008]. GRACE measures mass redistribution on the Earth by monitoring very precisely the distance between the two satellites and by tracking their positions via the GPS constellation. Changes in mass distribution (due to movement of water, air, and other sources) alter Earth's gravity field and change the distance (range) and speed (range-rate) between the satellites. Changes in the range of  $\sim 2 \mu\text{m}$  over the  $\sim 200 \text{ km}$  separation are detectable. This yields sensitivity to mass change equivalent to a  $\sim 1 \text{ cm}$  thick disk of water at the land surface, with dimensions of a few hundred kilometers or larger. Numerous studies have demonstrated that with this sensitivity, GRACE can contribute usefully to understanding total water storage changes in large basins with dimensions of many hundreds to thousands of kilometers. However, as the spatial scale of interest approaches a few hundred kilometers, GRACE data are more difficult to use. The goal of this study was to assess methods of estimating changes in water storage from GRACE data when the area of interest is near this resolution limit.

[5] GRACE responds to all sources of mass redistribution near the Earth's surface. Thus, it is important to correct measured range-rate variations for well-recognized influences, which include atmospheric mass redistribution, ocean mass redistribution due to currents and winds, ocean and solid Earth tides, and others. These mass redistributions are estimated from climate, ocean, and other models, and the associated mass variations are known as "dealiasing products" [Bettadpur, 2007]. Because dealiasing products are imperfect, new data releases (currently Release 04) have been computed over time to take advantage of improvements in dealiasing elements (e.g., the ocean tide model). Each release involves reprocessing all the range-rate data since launch in 2002, usually leading to demonstrable improvements in quality. The residual range-rate signal (after removing dealiasing products and effects of the solid Earth gravity field) should be due largely to terrestrial water storage variations, including ice storage change in polar areas and other effects, such as rebound of previously glaciated regions and earthquakes.

[6] Two types of products have been developed from GRACE range-rate data. One is a spherical harmonic (SH) expansion of the gravity field, analogous to a Fourier series representation for spherical geometry. Dimensionless coefficients of the expansion (Stokes coefficients) are the standard GRACE Level 2 product used in this study. Several sets of Stokes coefficients, reflecting varying computational strategies, are available at the official data repository online at <http://podaac.jpl.nasa.gov/grace/> (CSR, GFZ, JPL), and more recently from additional sources such as DEOS (<http://www.lr.tudelft.nl/live/pagina.jsp?id=6062b504-715e-4a22-9e87-ab2231914a4b&lang=en>), ITG (<http://www.geod.uni-bonn.de/itg-grace03.html>) or CNES/Groupement de Recherche en Géodésie Spatiale (GRGS) (<http://bgi.cnes.fr:8110/geoid-variations/README.html>). A second type of GRACE product translates range-rate residuals directly into a global set of localized surface mass concentrations ("mascons"), omitting the direct use of spherical harmonics [Rowlands *et al.*, 2005].

Mascon solutions are not examined in this study but are compared with SH solutions by Klees *et al.* [2008a].

[7] Changes in Stokes coefficients from month to month allow computation of maps of spatial water mass variations  $\hat{S}$  [see, e.g., Wahr *et al.*, 1998, Chambers, 2006]. The limited range of SH Stokes coefficients (typically to degree and order 60) fundamentally limits spatial resolution. Furthermore, noise contamination generally increases with increasing degree and order; therefore, those coefficients most important for fine spatial resolution are the noisiest. Thus, a compromise is needed to meet dual goals of noise suppression and maximum spatial resolution. A main point of this study is to examine various approaches to this compromise by finding combinations of available SH terms that are optimal by various measures.

## 2. Basin-Scale Studies and Associated Bias and Leakage

[8] Stokes coefficients,  $C_{l,m}$  and  $S_{l,m}$  relative to degree  $l$  and order  $m$  are generally estimated up to degree and order  $L_{\text{max}} = 60$ . This limit fixes spatial resolution at  $\sim 300 \text{ km}$  (in SH expansions, spatial resolution is typically reported as  $\pi a/L_{\text{max}}$ , where  $a$  is Earth radius). However, additional filtering is required to suppress increasing noise with increasing SH degree, leading to spatial resolution somewhat  $< 300 \text{ km}$ . A SH expansion of GRACE water storage variations can be displayed as a global map of month-to-month apparent surface mass changes, but these cannot be simply interpreted pixel-by-pixel as is done with traditional remote sensing images. Instead, comparison with independent observations or models must be made at the same spatial resolution by representing these observations as SH expansions with the same  $L_{\text{max}}$  and then applying the same filtering used with the GRACE data. Comparisons have generally been conducted in continental scale studies [e.g., Syed *et al.*, 2008]. Careful attention must be paid when estimating basin-scale water storage as described in this section.

[9] A surface mass change estimate for a space-limited region of interest  $R$  with area  $R_0$  requires a basin function  $h$  (Figure 1b), which is defined as 1 inside  $R$  and 0 outside the basin, i.e.,

$$h(X) = \begin{cases} 1 & \text{if } X \in R \\ 0 & \text{if } X \in \Omega - R \end{cases}$$

where  $X$  is position on the Earth's surface  $X = (\theta, \phi)$ , and  $\Omega$  represents the entire Earth surface. If  $L_{\text{max}}$  approaches infinity, the basin function approaches its ideal shape, but for finite  $L_{\text{max}}$  it is only an approximation to the exact  $h(X)$ . The GRACE water storage estimate  $\hat{S}_0$  over the region of interest of area  $R_0$  is then  $\hat{S}_0 = \frac{1}{R_0} \int_{\Omega} \hat{S} h d\Omega$  [Wahr *et al.*, 1998].

[10] A basin function can be described either on the Earth's surface or in terms of SH coefficients  $h(X) \rightarrow (h_{l,m}^c \text{ and } h_{l,m}^s)$ ; therefore, the estimate can also be written as a linear combination of the GRACE Stokes coefficients [Swenson *et al.*, 2003]:

$$\hat{S}_0 = \frac{4\pi a^3 \rho_e}{3R_0} \sum_{l=0}^{L_{\text{max}}} \sum_{m=0}^l \frac{2l+1}{1+k_l} (C_{l,m} h_{l,m}^c + S_{l,m} h_{l,m}^s),$$

where  $\rho_e$  represents the Earth's mean density. The weighting factor  $\frac{2l+1}{1+k_l}$  accounts for the Earth's response to surface mass

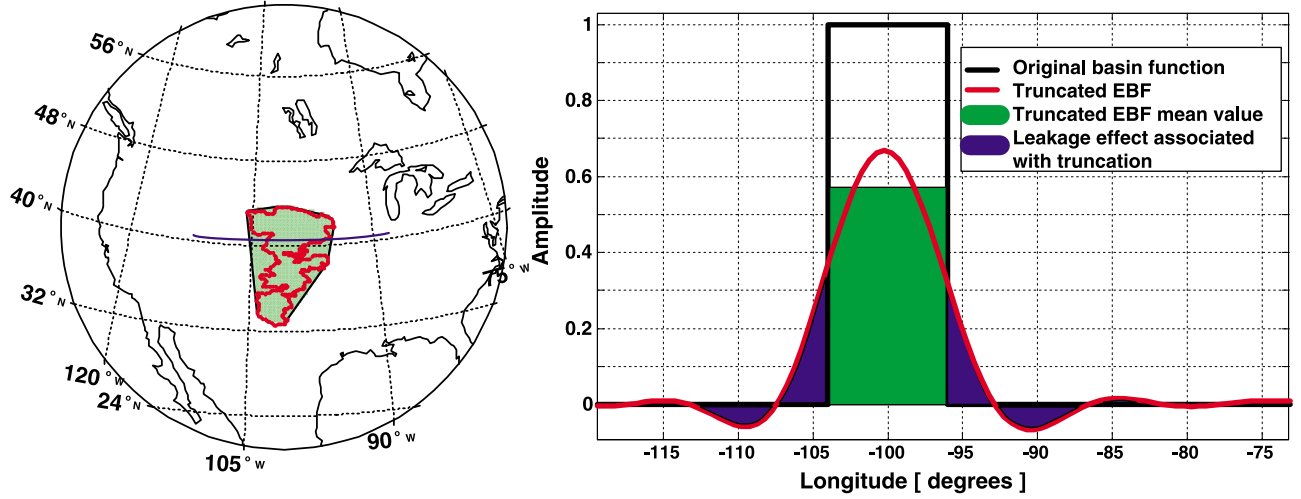


**Figure 1.** (a) Outlines of the High Plains aquifer (red) and of the convex portion of the simple basin function (black). (b) Cross-section of basin function near latitude 41 (black). Basin function truncated to maximum degree  $L_{\max} = 60$  (red). EBF, effective basin function.

loads at each SH degree, including both direct Newtonian attraction and elastic deformation via the load Love numbers  $k'_l$ , derived from seismic Earth models such as the preliminary reference Earth model [Dziewonski and Anderson, 1981] after solving gravitoelasticity equations [Pagiatakis, 1990; Guo et al., 2004].

[11] Because water storage estimates can be expressed as a set of linear weights applied to the Stokes coefficients, these estimates can be developed with the goal of both maximizing resolution within the region of interest and filtering high-degree and high-order Stokes coefficients to suppress noise (Figure 1b) [Swenson and Wahr, 2002]. The effective basin function (EBF)  $\hat{h}$  is defined as the spatial function on the surface of the sphere, and its corresponding SH weights are applied to GRACE Stokes coefficients developed with these two goals in mind.  $\hat{h}$  describes the ability of GRACE to determine an average water storage change within the basin of interest. There is more than one way to select the EBF  $\hat{h}$ , and a main goal of this study was to investigate how the EBF affects estimates of water storage variations.

[12] In practice, SH truncation and filtering associated with  $\hat{h}$  modifies the basin shape. An example is shown in Figure 1b, illustrating two differences relative to the exact basin function  $h$ . First, the mean value of the EBF over the basin of interest is no longer unity (which would lead to a biased estimate), and the EBF is not zero outside the basin, making the estimates sensitive to water storage changes outside the basin of interest (leakage). Bias and leakage time series may be calculated numerically considering the EBF  $\hat{h}$  [Klees et al., 2007]:  $\bar{S}_0 = \hat{S}_0 + \text{bias} - \text{leak}$  where

$$\text{bias} = \frac{1}{R_0} \int_R S_0 (h - \hat{h}) d\Omega \quad (1)$$

$$\text{leak} = \frac{1}{R_0} \int_{\Omega - R} S_{\text{leak}} \hat{h} d\Omega, \quad (2)$$

where  $S_0$  is true stored water variation and  $\bar{S}_0$  is average stored water over  $R$ .  $S_{\text{leak}}$  is true stored water variation outside the basin, and  $\hat{S}_0$  is the GRACE estimate before bias and leakage corrections. Note that the terminology used here differs somewhat from other studies. For example, Wahr et al. [1998] and Swenson and Wahr [2002] considered “leakage” to include effects of both bias (here associated with variations within the basin) and variations external to the basin (Figure 1b).

[13] Bias and leakage effects depend on actual water storage variations (both interior and exterior to the basin) and must generally be estimated from hydrological models. There is more than one way to select the EBF  $\hat{h}$ , and a main goal of this study was to investigate how the EBF affects estimates of water storage variations. The quality of the EBF may be measured by concentration near unity (ability to describe the area of interest) and rejection of contributions from surrounding areas (i.e. reducing leakage effects). EBF concentration is defined as follows:

$$\Lambda = \frac{\int_R \hat{h}^2 d\Omega}{\int_{\Omega} \hat{h}^2 d\Omega}, \quad (3)$$

the integrated squared value within the basin of interest relative to the globally integrated squared value. For example, a concentration of 0.9 means that only 10% of the variance (energy) originates from outside of the region of interest.

[14] Chen et al. [2005] showed that bias can generally be corrected to within a few percentage points using a simple multiplicative factor to rescale GRACE water storage estimates assuming a uniform distribution of water over the basin and no water storage variation outside the basin. The multiplicative factor  $k$  is then as follows:

$$k = \left( \frac{1}{R_0} \int_R \hat{h} d\Omega \right)^{-1}, \quad (4)$$

**Table 1.** Synthesis of Bias and Leakage Correction Methods<sup>a</sup>

Method	Assumption
Same processing applied to GRACE and a priori hydrological model	Fully trusts a priori hydrological model relative amplitude between inside and outside the basin of interest (i.e. spatial patterns). Model error damped by $(h - \hat{h})$ . Generally expressed as a single multiplicative coefficient.
Equation (1) + Equation (2) $bias = \frac{1}{R_0} \int_{\Omega} S_0 (h - \hat{h}) d\Omega \text{ and } leak = \frac{1}{R_0} \int_{\Omega-R} S_{leak} \hat{h} d\Omega$	Partly trusts a priori hydrological model relative amplitude over $(h - \hat{h})$ . Model error damped by $(h - \hat{h})$ . Bias and leakage contributions are calculated separately. Corrections expressed as time series.
Equation (4) + Equation (2) $k = \left( \frac{1}{R_0} \int_{\Omega} \hat{h} d\Omega \right)^{-1} \text{ and } leak = \frac{1}{R_0} \int_{\Omega-R} S_{leak} \hat{h} d\Omega$	No a priori for water mass variations inside the area of interest except homogeneity, trusts a priori hydrological model amplitude outside the area of interest. Model error damped by $(h - \hat{h})$ . Required when the a priori model does not fully model water storage variations (e.g., groundwater system) or when studying localized phenomena. Leakage correction expressed as time series.

<sup>a</sup>GRACE, Gravity Recovery and Climate Experiment.

according to the work by *Fenoglio-Marc et al.* [2006], *Velicogna and Wahr* [2006], and *Swenson and Wahr* [2007]. A second approach to determine bias and leakage employs a hydrological model. From the model, an equivalent rescaling factor is calculated as the ratio of hydrological model water storage mean value over a basin to values determined from the basin region after truncation and filtering of GRACE Stokes coefficients.

[15] Leakage arises from hydrological conditions outside the basin and is not generally described by a single multiplicative factor. Bias and leakage correction methods are summarized in Table 1, highlighting the different assumptions. *Rodell et al.* [2009] emphasized the importance of adapting bias and leakage estimation methods to a particular basin and estimated water storage variation. Recently, *Baur et al.* [2009] proposed an iterative process using forward modeling to correct for both bias and leakage.

[16] If temporal water storage variations are spatially homogeneous over a large area, bias and leakage partially cancel one another and filtered GRACE solutions may agree quite well with unfiltered estimates of water storage from hydrological models [*Chen et al.*, 2005]. Leakage effects tend to be reduced for basins near oceans, where storage variations are generally smaller, with the result that the bias effect may cause filtered GRACE data to significantly underestimate water storage variations in the basin. Additional leakage

problems have been observed for adjacent basins whose storage changes are out of phase (e.g., the Orinoco and Amazon basins).

[17] The different processing steps to estimate GRACE water storage variations at basin scale are synthesized in Figure 2. There were two main objectives in this study. The first (section 3) was to survey methods for estimating water storage variations considering problems of bias, leakage, and GRACE error, especially for basins with spatial dimensions near the limit of GRACE resolution, between ~450 and 750 km, and to determine the best concentration/filtering method that minimizes GRACE error and leakage correction error. A number of previously published approaches were surveyed and compared with an optimal concentration method on the basis of spatio-spectral localization [*Simons et al.*, 2006]. The second objective (section 4) was to derive and then apply the best suited method minimizing both GRACE error and leakage correction error for the particular case of the High Plains Aquifer (HPA) in central North America (Figure 1), a major groundwater resource. The HPA provides an interesting and useful test case to evaluate methodologies because of its size, irregular shape, and availability of detailed surface and groundwater monitoring. To supplement in situ observations, leakage effects were quantified using a numerical data-assimilating water storage model. Results from this study are important for testing the appli-

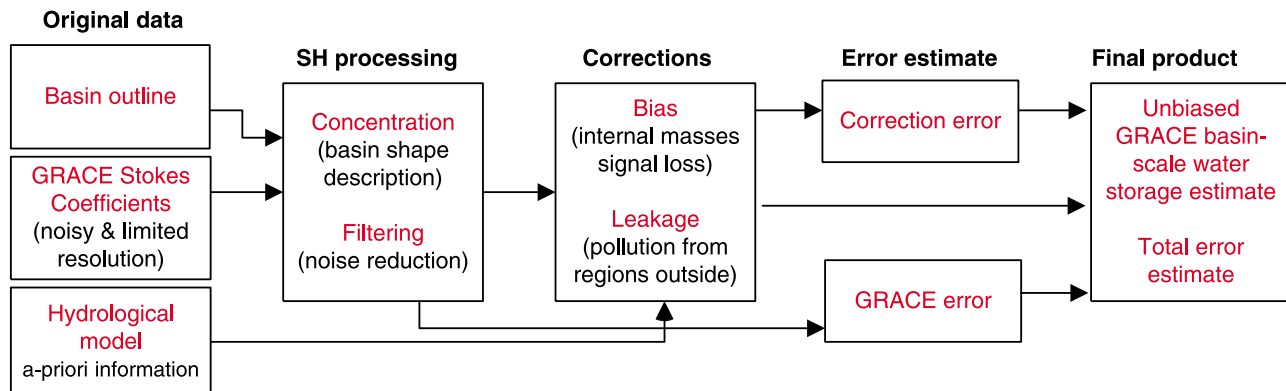


**Figure 2.** Diagram synthesizing the Gravity Recovery and Climate Experiment (GRACE) satellite processing for basin-scale water storage estimate on the basis of level 2 spherical harmonics products.

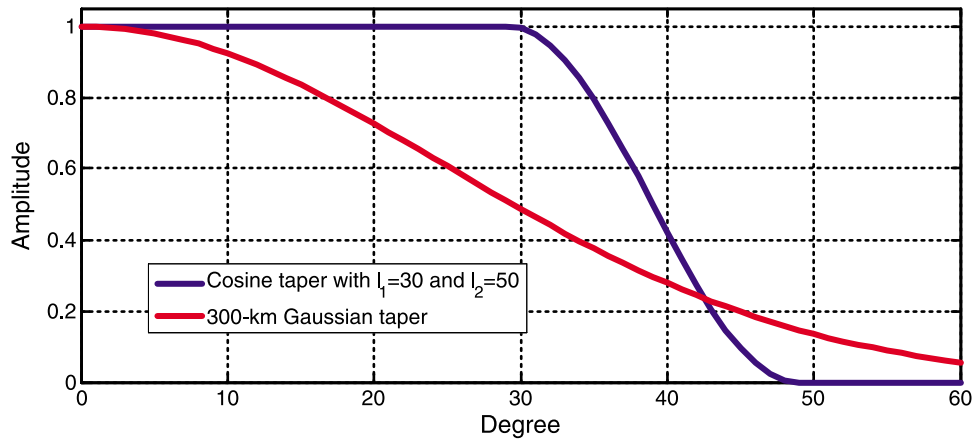


**Figure 3.** Transfer function of isotropic spherical harmonic (SH) filters used in this study, a 300-km gaussian filter, and cosine taper from degrees 30 to 50.

cability of GRACE to other areas of similar size and irregularity in shape.

### 3. Filtering and Construction of the Effective Basin Function

[18] Construction of GRACE changes in water storage typically involves two steps. The first is to filter GRACE data to suppress noisy high-degree and high-order SH coefficients, and the second is to find an effective basin function  $\hat{h}$  best concentrated within the region of interest considering a limited range of SH. These steps are treated separately in this study, although they are not completely independent. Filtering affects concentration by removing signal at high degrees and orders, as shown by *Chen et al.* [2007], and concentration may improve the signal-to-noise ratio by limiting noise leakage into the region of interest [*Han et al.*, 2008]. The quest to find the optimal filtering and concentration methods depends on the nature of the noise, size, and shape of the region of interest, and to some extent the hydrological setting of the region. Therefore, solutions need to be tailored to the region of interest. Three parameters are listed to measure the quality of an EBF. The first two depend only on geometrical properties of the region of interest: (1) the EBF concentration  $\Lambda$  and (2)  $b = k^{-1}$ , the mean value of the EBF over the region of interest (the reciprocal bias). The third parameter measures the efficiency of investigated methods: the final error  $\Delta\bar{S}_0$  on GRACE basin-scale water storage estimate after bias and leakage corrections.

#### 3.1. Filtering to Suppress GRACE Measurement Noise

[19] Two types of filters for suppression of noisy SH coefficients are in general use: (1) fixed parameter filters and (2) data adaptive filters (i.e. filters that adjust their transfer functions according to an optimizing algorithm). Fixed parameter filters include isotropic gaussian (applied equally to all orders at each degree) [*Jekeli*, 1981; *Wahr et al.*, 1998] and cosine taper or anisotropic filters [*Wooters et al.*, 2007]. Data-adaptive filters may use geophysical models or GRACE observations to judge noise and signal levels. These may be isotropic or anisotropic [*Guo et al.*, 2010; *Han et al.*, 2005; *Sasgen et al.*, 2006; *Seo et al.*, 2006; *Swenson and*

*Wahr*, 2006; *Kusche*, 2007]. Additional examples include the adaptive filter of *Klees et al.* [2008b], which minimizes RMSE while accounting for signal variance and covariance and the iterative least squares filter to pass signal and reject noise using a priori water storage estimates from hydrological models [*Ramillien et al.*, 2005].

[20] Besides suppression of noisy high-degree Stokes coefficients, another important problem is suppression of longitudinal stripes found in most current GRACE solutions. These stripes are due to the ill-posed nature of the least squares estimation problem [*Save*, 2009] and to aliasing of geophysical signals at time scales  $<1$  month [*Seo et al.*, 2008]. *Swenson and Wahr* [2006] developed an effective data-adaptive polynomial filter to remove the stripes. It is possible that future GRACE product releases will suppress these stripes. A modified version of the *Swenson and Wahr* [2006] destriping filter was applied in this study. A fourth-degree polynomial was fit for SH orders 6 to 40. Above SH degree 40, the polynomial degree was reduced to 3 up to degree 50.

[21] The performance of the following common fixed-parameter filters was examined. An isotropic gaussian filter, expressed by coefficients  $W_l$  for all orders of SH of degree  $l$ :

$$W_l = \exp\left(-\frac{(lr)^2}{4 \ln(2) a^2}\right),$$

where  $r$  is the half-length radius of the filter (Figure 3). *Sasgen et al.* [2006] showed that the optimal isotropic Wiener filter is close to a gaussian filter with a 400 km half radius. An isotropic cosine taper, also defined in the SH domain by the following (Figure 3):

$$W_l = \begin{cases} 1 & \text{if } l < l_1 \\ \frac{1}{2} \left(1 + \cos\left(\pi \frac{l-l_1}{l_2-l_1}\right)\right) & \text{if } l_1 < l < l_2 \\ 0 & \text{if } l > l_2 \end{cases}$$

The half-length wavelength is defined as  $\frac{2\pi a}{(l_1+l_2)}$ . The cosine taper has the advantage of suppressing only the highest SH degrees, leaving mid-degrees unchanged. The bandwidth is also better limited, suppressing entirely SH degrees above  $l_2$ .

### 3.2. Construction of the Effective Basin Function

[22] The purpose of EBFs is to best describe the area of interest considering the maximum degree  $L_{\max}$  of GRACE products. No EBF can be strictly both space-limited and band-limited to a range of SH coefficients below  $L_{\max}$  [Percival and Walden, 1993]. Although space-limited methods may be seen as most adapted to examine specific regions of interest, truncation of the SH expansion to degree 60 affects their shape (Figure 1b). Methods that work directly with the SH coefficients are thus more suited to investigate water mass variations from GRACE associated with a localized geophysical phenomenon because they allow control over the useful range of Stokes coefficients.

[23] The simplest approach to the concentration problem is to truncate the exact basin function to the range of available SH. An east-west section through a simple truncated basin function ( $L_{\max} = 60$ ) is shown in Figure 1b, along with related statistics concerning bias and leakage. Simple truncation produces large oscillating side lobes outside the region of interest. Two modifications to this approach were also examined in this study. The first modification is to use a truncated function with the smallest convex region containing the basin of interest as indicated in Figure 1a. The MATLAB “convhull” function was used to select from the original contour the contour points describing the smallest convex shape. This simple geometric operation leads to smoothing of complicated basin shapes and increases the amplitude of low- and mid-SH degrees relative to simple truncation. The second modification is to use a Hamming Window instead of sharp truncation of Stokes coefficients. This reduces side lobes outside the region of interest. Simple truncation and the two modifications depend entirely on the geometry of the region of interest.

[24] A data-adaptive method developed by Swenson *et al.* [2003] aims at minimizing the sum of GRACE error and leakage error. This method is neither space-limited nor band-limited (except if GRACE errors are considered as infinite for  $l \geq L_{\max}$ ), but it has the important characteristic of damping noisier high-degree SH's. The isotropic modification of the basin function leads to  $\hat{h}_{lm} = \left(1 + \frac{2B_l^2}{(2l+1)\sigma_0^2 G_l}\right)^{-1} h_{lm}$ , where  $B_l$  values are degree amplitudes of GRACE measurement errors given in terms of an equivalent water layer,  $G_l$  values are Legendre coefficients of an assumed exponentially decaying signal spatial covariance function, and  $\sigma_0^2$  is signal variance. This EBF is generally insensitive to the correlation length of the signal covariance function, and a value of 500 km was used in this study, in the midrange of that suggested by Swenson *et al.* [2003]. This is referred to as Swenson's EBF in the following discussion. GRACE error is taken as the formal error provided by GRACE processing centers. Because formal error likely underestimates true error, Swenson's window is used in combination with other filters that suppress high SH coefficients. This window would perform optimally using realistic error estimates, which are not necessarily reported with GRACE products from the various processing centers.

[25] Recently, new methods for SH analysis, called spatio-spectral localization, have been developed to maximize the concentration parameter  $\Lambda$  [Simons and Dahlen, 2008]. This work follows from Fourier time series analysis results from Slepian [1978], leading to multitaper spectral analysis

methods [Thomson, 1982]. The idea is to find, for maximum SH degree  $L_h$ , functions that maximize the concentration  $\Lambda$  from equation (3). Wieczorek and Simons [2005] derived this result for axisymmetric windows and it was extended to arbitrary domains by Simons *et al.* [2006]. There is a set of functions  $\hat{h}$  that maximize  $\Lambda$ , and all are eigenvectors of the eigenvalue problem  $D\hat{h} = \lambda\hat{h}$ , where matrix  $D$  contains integrals of products of Legendre polynomials. The resulting set of Slepian functions  $\hat{h}$  are orthogonal over both the entire sphere and on the region of interest. Among the  $(L_h + 1)^2$  solutions to this equation, only well-concentrated solutions ( $\lambda \approx 1$ ) are used. The number  $N$  of well-concentrated solutions  $\hat{h}$  is found from the equivalent of the Shannon number on a sphere,  $N = (L_h + 1)^2 \frac{R_0}{4\pi a^2}$ , which is the product of the SH bandwidth and the normalized area of the basin of interest [Simons *et al.*, 2006].  $L_h$  may be chosen to be as large as  $L_{\max}$ . However, in practice,  $L_h$  is maintained as small as permitted by the size of the basin. The goal is to achieve a balance between spatial and spectral concentration [Dahlen and Simons, 2008] and to limit noise contamination from GRACE high-degree SH coefficients. The final EBF is built as the sum of the chosen  $N$  well-concentrated  $\hat{h}$ .

### 3.3. GRACE Noise Levels

[26] Numerous studies of GRACE errors have been published. Wahr *et al.* [2004] and Seo *et al.* [2006] provide overviews of the GRACE error budget in water storage estimates using GRACE Release 1 (RL01) solutions. For a given month, RMSE values are typically in the range of 5 mm (equivalent water thickness) for the fundamental GRACE measurement (satellite to satellite range rate) and 10 to 50 mm for errors in atmospheric and oceanic corrections, depending on latitude. GRACE measurements tend to be more precise at high latitudes owing to increased track density associated with a polar orbit, but atmospheric and oceanic dealiasing products typically degrade in quality at higher latitudes [Seo and Wilson, 2005]. Wahr *et al.* [2006] proposed an estimate of error from nonseasonal GRACE residuals over land, after subtracting annual and semiannual sinusoids and smoothing, but this approach tends to overestimate errors when there are significant nonseasonal signals. Chen *et al.* [2009] estimated errors from residual variations over the oceans, taking into account atmospheric effects not in dealiasing products. Deficiencies in oceanic dealiasing products might cause this error estimate to be too large as well. However, both error estimates are similar, with RMSE values  $\sim 25$  mm (equivalent water layer thickness) depending on the latitude of the basin.

[27] Concentration effects (i.e. bias and leakage correction errors) should also be considered when focusing on a space-limited area. In the following, bias is assumed to be corrected using the multiplicative factor  $k$ , which implies spatially homogeneous variations within the basin. For simplicity in estimating leakage correction error, mass variations outside the area of interest are also considered as spatially homogeneous with amplitude  $S_{leak}$  in the region of sensitivity of the EBF. Leakage can then be rewritten as  $leak = \beta S_{leak}$  with  $\beta = \int_{\Omega} \hat{h} d\sigma$ . Finally, the total error  $\Delta\bar{S}_0$  may be written as  $\Delta\bar{S}_0 = k \Delta\hat{S}_0 + \hat{S}_0 \Delta k + \Delta(k\beta) S_{leak} + k\beta \Delta S_{leak}$ . Total error is the sum of the following:

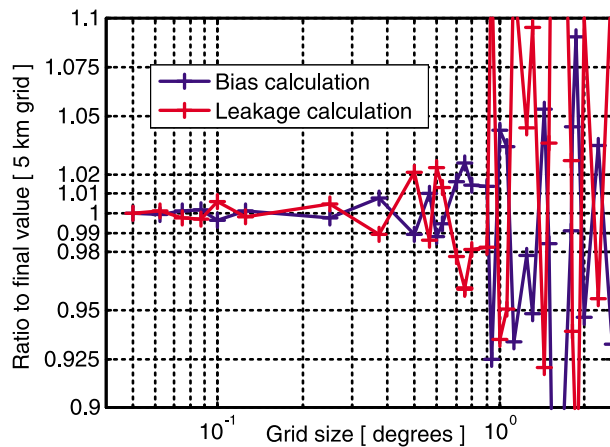


**Figure 4.** Convergence on bias and leakage calculation with respect to grid size for the High Plains Aquifer (HPA).

[28] (1)  $k \Delta \hat{S}_0$ , level 2 GRACE error estimate amplified by bias correction. The methodology of *Chen et al.* [2009] was used in this study to estimate  $\Delta \hat{S}_0$ . RMS variability was calculated over all oceans in a latitudinal band containing the basin but excluding ocean regions within 1000 km of continents to avoid leakage from terrestrial storage changes. Over an area equivalent to the High Plains Aquifer, the error  $\Delta \hat{S}_0$  is on the order of 10 mm using a 300-km gaussian smoother for GRACE data measured after 2002.

[29] (2)  $\Delta k \hat{S}_0 + \Delta(k\beta)S_{leak}$  is the calculation error in estimating bias and leakage effects. It includes both numeric errors in integral calculation and error in approximating the basin using rectangular grids. With 0.25-degree grid resolution, this error is <1% (Figure 4), and with 0.5-degree grid this error is <2%. A similar grid for a hydrological model would accurately correct leakage effects.

[30] (3)  $k\beta \Delta S_{leak}$  is the error due to leakage correction, which is derived from a hydrological model and linked to the concentration parameter. This error is difficult to evaluate because it requires an error estimate from an a priori hydrological model. As a first guess, a standard deviation from differences among VIC, MOSAIC, CLM, and NOAH land surface models, included in Global Land Data Assimilation Systems (GLDAS) [Rodell et al., 2004a], was used. Unfortunately, all models in GLDAS use the same forcing dataset; therefore, errors are probably correlated, and the resulting value of 30 mm may thus be an underestimate.

#### 4. Application to the High Plains Aquifer

[31] The unconfined High Plains Aquifer (HPA) (450,000-km<sup>2</sup> area) (Figure 1a) is the principal source of water for one of the major agricultural areas in the world in central North America. The climate of the region is mostly semiarid, with mean annual precipitation (P) ranging from 350 mm in the west to 750 mm in the east and mean annual temperature ranging from 7.5°C in the north to 18°C in the south [PRISM mean 1895–2008, www.prismoregonstate; Daly et al., 2008; DiLuzio et al., 2008]. Potential evapotranspiration greatly exceeds precipitation; therefore, agriculture in the region is heavily dependent on irrigation, mainly from groundwater [McGuire, 2007]. The HPA was specifically mentioned in the National Research Council report

“Satellite Gravity and the Geosphere” as suitable for study with a satellite system such as GRACE [Dickey et al., 1997], and a prelaunch study by Rodell and Famiglietti [2002] confirmed this. Since then, Strassberg et al. [2007, 2009] verified that GRACE can monitor HPA water storage variations, showing that at seasonal time scales, GRACE data agree well with water storage estimates from ground-based measurements.

#### 4.1. Data and Processing

[32] Two different GRACE data sets were used to test the filtering and concentration schemes examined in this study. The first is monthly samples from the Center for Space Research (CSR) RL04 GRACE SH ( $L_{max} = 60$ ) [Bettadpur, 2007]. The second is 10-day samples produced by CNES-GRGS RL01 ( $L_{max} = 50$ ) [Lemoine et al., 2007]. GRGS solutions are stabilized so that the time-variable part of the Stokes coefficients diminish to 0 at degree 50. CSR and GRGS solutions use the same range-rate data and similar geophysical models but employ independent processing strategies. Therefore, it is interesting to compare results for the HPA using both.

[33] In all cases, total water storage variations from GLDAS NOAH [Rodell et al., 2004a], available on a 0.25-degree grid, was taken as the a priori hydrological model to correct for leakage effects. GRACE mass storage estimates were compared with GLDAS-NOAH predictions (monthly or 10-day averages) and with water storage variations derived from groundwater table elevations and soil moisture point measurements and analyzed by Strassberg et al. [2009]. The soil moisture and groundwater data were also analyzed at a daily time step using the Karhunen-Loeve transform to extract significant modes of spatial and temporal variability from the point measurements. Kriging was then performed on the spatial pattern associated with each mode to calculate a spatial mean. The details of this modal upscaling analysis are beyond the scope of this paper and can be found in the work by Longuevergne et al. [2007]. The resulting time series is, however, given as an alternative to that of Strassberg et al. [2009]. They calculated mean soil moisture variations over a 1-degree grid when data were available. A seasonal signal was assumed to calculate groundwater storage variations and determined using available data. Differences between the two estimates provide a measure of uncertainty in water storage estimates derived from the point measurements. At monthly time scales, the variance of the mode-derived time series is reduced relative to that of Strassberg et al. [2009] by 8%, and the correlation between the two analyses is 0.92.

#### 4.2. Comparison of Concentration Methods

[34] Five different EBFs have been used to estimate HPA water storage variations from GRACE (Figure 5). In the case of the Slepian EBF, the maximum degree and order was set at  $L_h = 50$  and the first two solutions to the eigenvalue problem  $D\hat{h} = \lambda\hat{h}$  were used to describe the elongated shape of the HPA. Experimentation with a large value  $L_h = 60$  (a possibility with the CSR solution) would allow computing an EBF on the basis of the first three solutions and better describe the shape of the HPA. However, this choice did not significantly improve concentration and reciprocal bias; therefore, using the full range of Stokes coefficients avail-

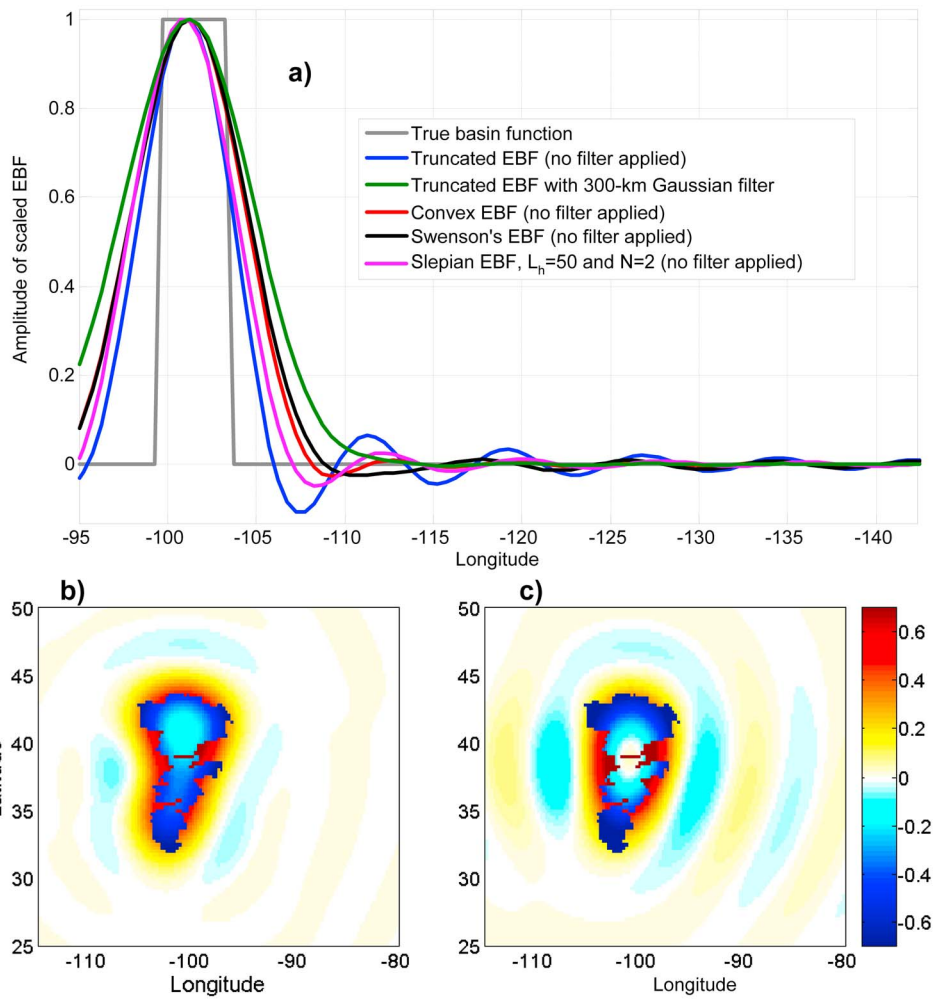


**Figure 5.** a) Comparison among several EBFs for the HPA at latitude 40°N. SH expansion maximum degree is 60. The *Slepian* [1978] EBF is the sum of the first two eigenvectors, with  $L_h = 50$ . Differences between EBFs and the true basin  $\hat{h} - h$  for (b) Swenson's EBF and (c) Slepian's EBF.

able with the CSR solution would not be optimal in terms of final error.

[35] Leakage problems are illustrated after rescaling the EBF to restore the signal amplitude (Figure 5a). Side lobe oscillations are partially damped by gaussian filtering. Other

methods besides the truncated basin function, including the convex truncated basin function, are less subject to oscillation problems. When a filter is applied, the EBFs converge more quickly toward 0 outside the area of interest.

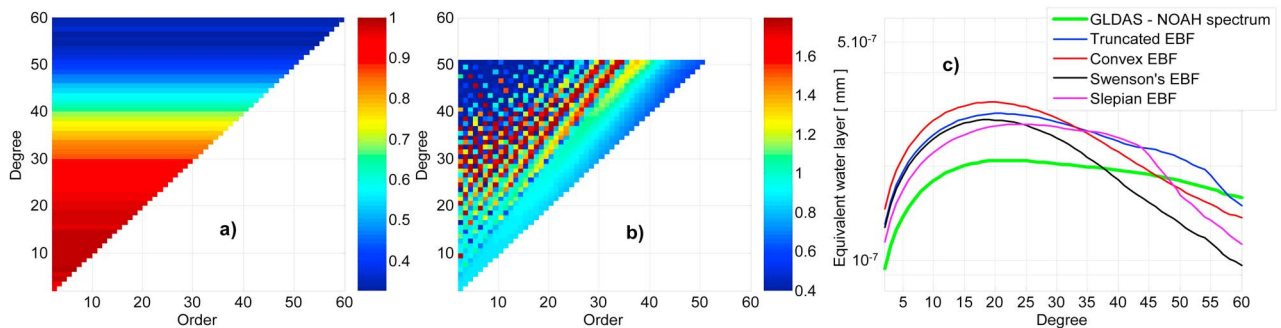


**Figure 6.** Spectrum characteristics of EBFs. (a) Swenson's EBF; (b) Slepian's EBF, both relative to the exact basin function; and (c) RMS amplitude spectra of GRACE estimates as a function of SH degree after a 300-km gaussian filter and bias correction are applied.

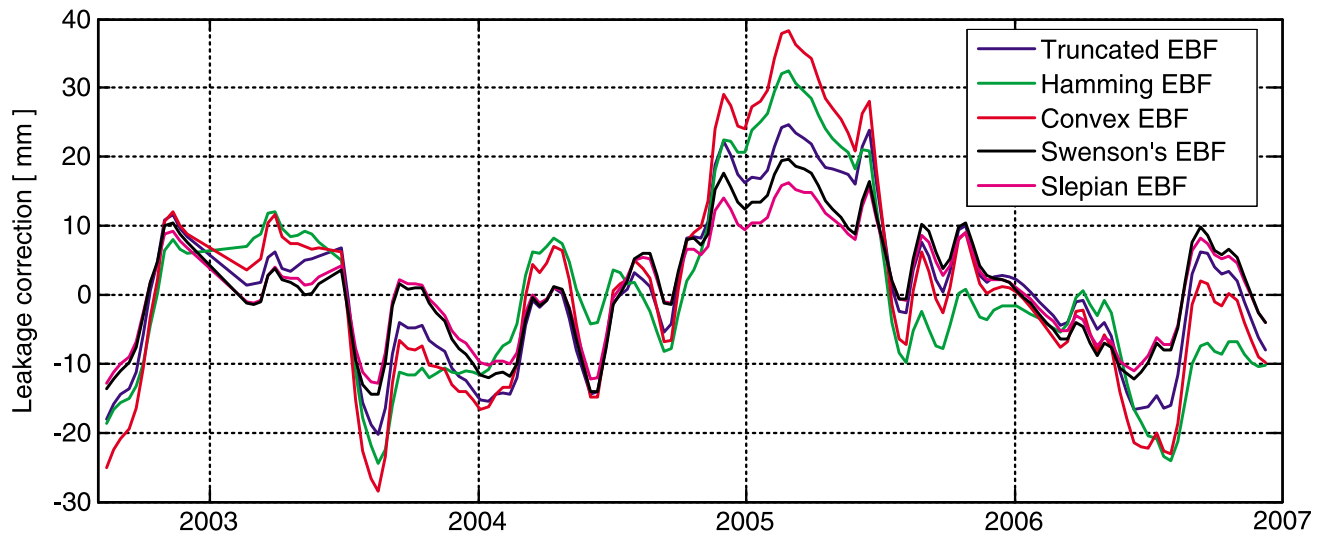


**Figure 7.** Leakage effect associated with various concentration methods after a cosine taper between degree 30 to 50 is applied, considering Global Land Data Assimilation Systems (GLDAS) -Noah stored water variations (snow, vegetation and all soil moisture layers) as a-priori information.

[36] The difference between the EBF  $\hat{h}$  and the true basin  $h$  was used to evaluate bias and leakage effects (Figures 5b and 5c). The fact that the EBF is not homogeneous over the entire region of interest should be taken into account, especially for irregularly shaped basins such as the HPA.

[37] The five EBFs have different characteristics affecting the SH spectrum of the solution (Figure 6). Swenson's EBF damps the highest-degree coefficients to reduce Stokes coefficient errors that increase with degree. In contrast, the convex function amplifies the highest degrees and diminishes the lowest degrees (Figure 6c). Because the Slepian EBF is derived by an optimization process, it is not simply related to the exact basin function. At low degrees, EBFs are identical, but at higher degrees, specific degrees and orders are amplified or damped (Figure 6b).

[38] After windowing by the original basin function, the GLDAS spectrum diminishes slowly as SH degree increases (Figure 6c), but GRACE error limits the ability to recover these high degrees. Swenson's EBF, which uses the GRACE formal error spectrum, is likely the most effective in accounting for this. The Slepian EBF offers a trade-off among the EBFs, retaining mid-degrees to describe the basin shape while diminishing rapidly at higher degrees.

[39] Leakage correction requires knowledge of the signal exterior to the basin and was estimated on the basis of the GLDAS-Noah stored water variations (considering snow, vegetation, and soil moisture) for various EBFs (Figure 7). Swenson's EBF and Slepian's EBF reduce leakage below 15 mm most of the time. Leakage is also dependent on the filtering method.

[40] Bias was computed using both GLDAS-Noah as a priori information for true water storage inside the area of interest and the geometric multiplicative factor  $k$ . GLDAS-Noah-derived bias may then be expressed as an equivalent multiplicative factor by a least squares fit to uncorrected GRACE data (Table 1). Both estimates may differ by up to 40%. Indeed, GLDAS-Noah does not model groundwater storage variations and therefore significantly underestimates

true water storage changes inside the HPA. For this reason, the SH approach described above was used to estimate the bias factor  $k$ .

#### 4.3. Noise Reduction–Spatial Resolution Trade-Off

[41] Error in GRACE water storage estimates is linked to both the EBF properties and to the filtering method. An unfiltered EBF may exhibit excellent concentration, but in combination with filtering, concentration is diminished with resulting increases in bias and leakage (Figures 8a and 8b). The destriping filter may have a large impact, because this filter removes variance similar in shape to the HPA, which trends north-south. However, the real impact of the destriping filter is difficult to determine accurately. The destriping filter is data-adaptive (i.e., not a conventional linear filter) and fitted to GRACE data directly; therefore, predicting its effect cannot be undertaken by destriping the shape of the aquifer or results from hydrological models. In practice, as shown in Tables 2 and 3 and Figure 8, the amplitude of CSR time series is very close to that of the GRGS time series (which does not require any destriping) and to that of ground data. Therefore, destriping is assumed to have little effect on concentration and bias in the following analysis. GRACE error without destriping is as high as 50 mm most of the time, whereas use of the destriping filter reduces GRACE error by a factor of  $\sim 10$  (not shown in Figure 8c). This filter is thus absolutely necessary for CSR RL4 solutions. A cosine taper filter is an interesting alternative to the gaussian filter and reduces leakage problems by filtering the highest degrees only and leaving mid-degrees unchanged. It also has better spectral characteristics than the gaussian filter.

[42] Compared to a truncated basin function, the convex basin function decreases bias, showing that this simple geometric operation can be useful for smaller basins. However, it does not perform well for the HPA because of the indented shape of the HPA (its boundary is in places concave). Concentration is diminished as a result, leading to larger leakage.

**Table 2.** Filtering and Concentration Applied for GRACE Processing on the High Plains Aquifer

	Processing Applied	CSR Solutions	GRGS Solutions
HPa 450,000 km <sup>2</sup>	Filter method	Cosine taper [30 50]	No filter
	Concentration method	Slepian EBF N = 2 L <sub>h</sub> = 50	Slepian EBF N = 2 L <sub>h</sub> = 50
	Concentration $\Lambda$	0.60	0.66
	Multiplicative factor $k$	1.64 (1.23 using GLDAS-Noah)	1.45 (1.08 using GLDAS-Noah)
	RMS error	24 mm	26 mm
Northern part of HPa, 210,000 km <sup>2</sup>	Filter method	Cosine filter [40 60]	No filter
	Concentration method	Slepian EBF N = 1 L <sub>h</sub> = 50	Slepian EBF N = 1 L <sub>h</sub> = 50
	Concentration $\Lambda$	0.60	0.60
	Multiplicative factor $k$	2.0 (1.32 using GLDAS-Noah)	1.66 (1.10 using GLDAS-Noah)
	RMS error	30 mm	30 mm
Southern part of HPa, 240,000 km <sup>2</sup>	Filter method	Cosine filter [30 50]	No filter
	Concentration method	Slepian EBF N = 1 L <sub>h</sub> = 50	Slepian EBF N = 1, L <sub>h</sub> = 50
	Concentration $\Lambda$	0.55	0.58
	Multiplicative factor $k$	1.66 (1.29 using GLDAS-Noah)	1.47 (1.18 using GLDAS-Noah)
	RMS error	30 mm	30 mm

However, the leakage is more concentrated near the edge of the HPA compared to a simple truncated EBF. The Hamming EBF is generally inferior relative to the truncated or convex EBF. Swenson's EBF performs very well, providing high concentration despite the complicated shape of the HPA.

[43] For the CSR solution, the best combined concentration/filtering method is the Slepian EBF, supplemented by a cosine taper between degrees 30 and 50, which results in a final RMSE of ~25 mm. When using a 300-km Gaussian filter, GRACE error is higher (10 mm versus 7 mm); however, the leakage correction error is lower (~14 mm versus 18 mm). The optimum concentration/filtering method for the GRGS solutions is quite different because GRGS solutions are stabilized. Because of the lack of stripes in GRGS solutions, in contrast to CSR solutions, no additional filtering is optimum. Despite the GRGS  $L_{\max} = 50$ , GRACE error is higher (15 mm) but leakage correction error is reduced to 12 mm. The final chosen filtering/concentration methods are described in Table 2.

[44] When using the CSR solution for the HPA, the choice of filtering method to reduce noise is more critical than the concentration method. Most of the concentration methods lead to errors within 5 mm of one another. In contrast, the concentration method was more important for the GRGS solution, which does not require additional filtering for the HPA.

[45] Deriving basin scale water storage estimates using a truncated EBF does not lead to error estimates that are significantly higher. However, the sensitivity of truncated EBFs to external masses may extend quite a distance from the region (Figure 5), which is not properly translated here in the

leakage correction error estimate. As a result, leakage correction errors may be underestimated, especially in the case of large spatial variations in water storage (e.g., in monsoon areas). In the latter cases, the use of a *Slepian* [1978] window, by maximizing concentration, would minimize sensitivity to water masses outside the area of interest and thus, leakage error.

[46] GRACE error for deriving total water storage variations in both saturated and unsaturated zones is slightly lower than the GLDAS-Noah estimated error, which is limited to soil moisture variations. GRACE thus provides meaningful data to improve knowledge of the water cycle over the HPA and to recover groundwater storage variations (Figure 9).

#### 4.4. Water Storage Variations in the High Plains Aquifer

[47] The optimal combination of concentration/filtering was applied to extract stored water variations for the HPA. The selected processing scheme and the main characteristics are summarized in Table 1. CSR and GRGS solutions employ independent processing strategies and require different processing methods, but GRACE water storage estimates agree well (Figure 8), which provides confidence in the methodology and processing choices selected.

[48] Agreement between ground-based total water storage estimates and GRACE estimates is generally very good, except for the April 2003 peak. Correlations are  $\geq 0.8$  for CSR at monthly and seasonal time scales and  $\geq 0.70$  for GRGS solutions at 10-day time scales (Table 2). Although HPA is large, discharge from irrigation and evapotranspiration and recharge from precipitation are far from uniform

**Table 3.** Correlation and Amplitude Factor Between GRACE-Derived Water Storage Variations and Soil Moisture+Groundwater Analysis for Several Time Scales<sup>a</sup>

	CSR			GRGS			
	Cor. 30 d	Cor. 90 d	Fact.	Cor. 10 d	Cor. 30 d	Cor. 90 d	Fact.
HPA	0.80	0.87	1.18	0.70	0.71	0.77	1.12
HPA north	0.79	0.84	1.13	0.75	0.77	0.83	1.10
HPA south	0.80	0.88	1.12	0.75	0.78	0.87	1.12

<sup>a</sup>The amplitude factor is defined as the ratio between the standard deviations. Cor. stands for correlation and Fact. for amplification factor.

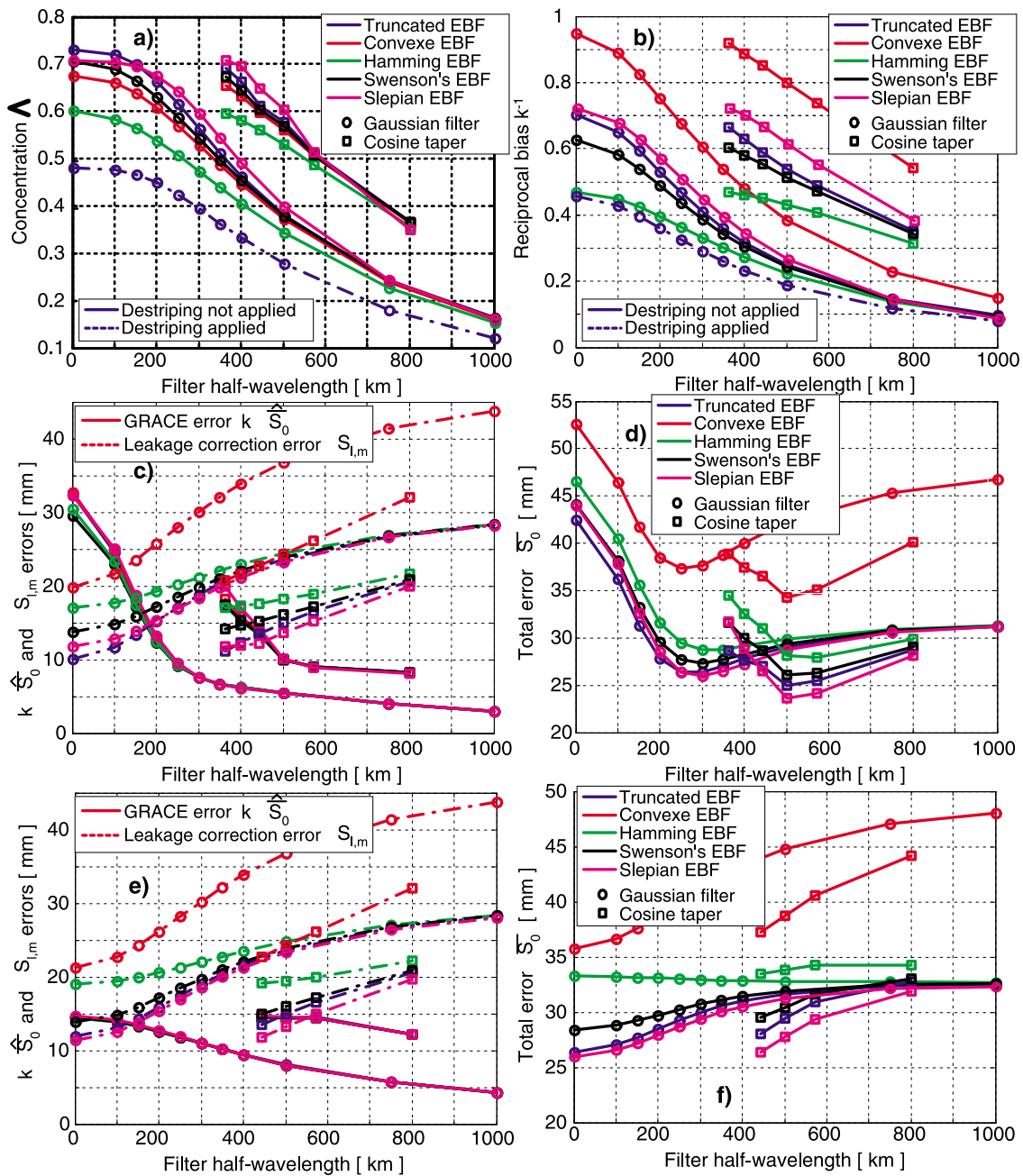


**Figure 8.** Variation of reciprocal bias, concentration, and final GRACE error estimate for the HPA as a function of the concentration method and the filtering method used (gaussian or cosine taper as a function of the filter half-width). Destriping effect is shown for a truncated basin function only. Maximum degree for SH expansion is 60. Slepian function is built as the sum of the two first tapers, the bandwidth being limited by  $L_h = 50$ . (a) Concentration; (b) mean value of EBF or reciprocal bias; (c) CSR GRACE error after destriping algorithm is applied and leakage correction error; (d) CSR total error; (e) GRGS GRACE error and leakage correction error; and (f) GRGS total error.

over the HPA, making spatial resolution a challenging issue. Moreover, the EBFs for the HPA as a whole are not homogeneous because of differential hydrological behavior and the elongated shape of the aquifer (Figures 6b and 6c); therefore, division into subregions should conform better to the homogeneity hypothesis assumed when using a simple scalar bias correction  $k$ . To test this idea, the aquifer has been sub-

divided into a northern part (210,000 km<sup>2</sup>) and a southern part (240,000 km<sup>2</sup>) by the 40th parallel. The northern and southern parts of the aquifer behave differently. For example, the 100 mm recharge event during September–October 2004 is restricted to the southern part of the aquifer (Figure 9). Correlation with GRACE estimates is retained for the sub-basin time series, which validates the concept of using

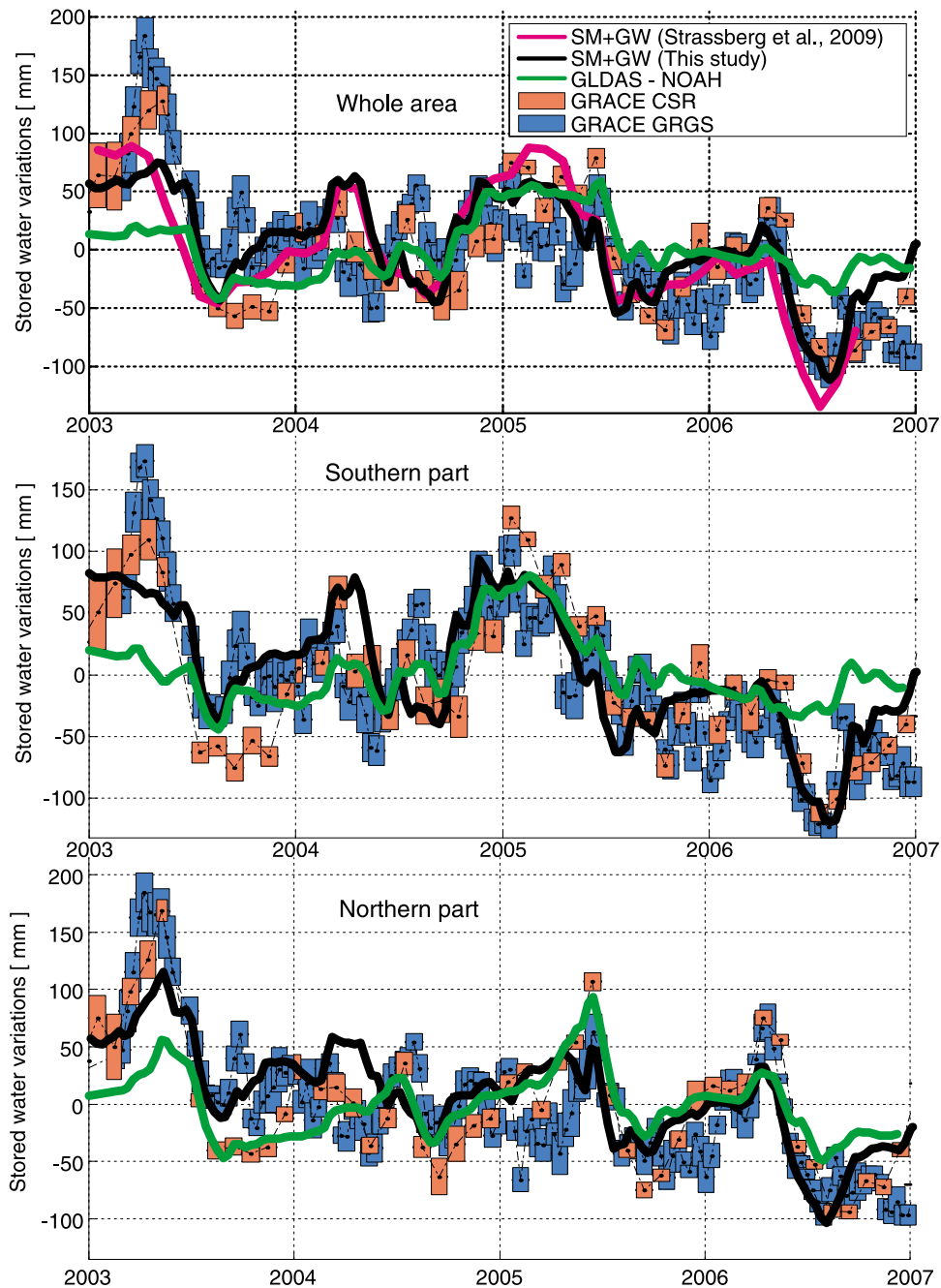


**Figure 9.** Comparison between GRACE-derived stored water variations for both CSR and GRGS solutions with water storage derived from ground-based measurements and GLDAS-Noah model. Only GRACE measurement error is shown for clarity, leakage correction error is excluded ( $\sim 13$  mm). SM and GW stand, respectively, for soil moisture and groundwater measurements.

GRACE to study regions at this scale. Note that the optimal filter for CSR solutions differs for the northern and southern parts of the aquifer.

[49] GRGS 10-day solutions provide improved monitoring of rapid water storage variations, such as those related to aquifer pumping during spring 2003 and spring 2006. Even if the correlation between GRACE and ground-based measurements is slightly lower compared to monthly sampling, its value ( $\geq 0.70$ ) at 10-day time scales indicates that

interesting information is available at shorter time scales than provided by the CSR solutions.

[50] In all cases, variance in GRACE water storage estimates exceeds that of ground-based water storage by 10%–18%. There are several potential explanations for this, including (1) overestimation of bias corrections using the simple multiplicative factor  $k$ , (2) underestimation of leakage corrections related to underestimation associated with the GLDAS-Noah water storage estimates, and (3) inadequate

ground measurements producing biased regional estimates. Strassberg *et al.* [2009] found closer agreement between GRACE and surface estimates with GRACE variance exceeding ground-based variance by 5%–10 %.

## 5. Summary

[51] This study investigated how different processing choices may affect GRACE level 2 estimates of water storage variations, considering problems of bias, leakage, and GRACE error when focusing on spatial scales near the limit of GRACE resolution, between ~450 and 750 km. Leakage correction in particular relies on an a priori hydrological model; therefore, leakage should be reduced to make GRACE water storage variations independent from a priori hydrological models. Spatiospectral concentration was introduced to minimize leakage effects. This method allows restriction of the spherical harmonic bandwidth to achieve a balance between spatial and spectral concentration, optimally describing the shape of the basin while avoiding noise contamination from noisy high degrees Stokes coefficients. Reliable estimates of water storage variations require a trade-off among GRACE noise reduction, maximum spatial resolution, and minimum spatial leakage, achieved by minimizing errors related to GRACE and leakage correction. Optimum filter type and concentration methods may vary from basin to basin, depending on geographical location, shape, characteristics of hydrological signals in and surrounding the basin, and also GRACE noise characteristics. As a result, the optimized method varies from region to region and should be determined separately for each basin and the particular GRACE solution.

[52] To increase confidence in derived methods, water storage variations were calculated for both CSR and GRGS solutions, which employ different processing strategies. The approach to developing a processing scheme in this study was validated for the High Plains Aquifer, where intensive monitoring of soil moisture and groundwater has been conducted. Using the CSR GRACE solution for small basins, the choice of filtering method is more critical than the concentration method. In contrast, the concentration method was more important for the GRGS solution, which does not require additional filtering in this case. In both cases, the Slepian [1978] window was found to be the most suitable method for deriving estimates of water storage variations from GRACE in a space-limited area. These windows are indeed optimized to reduce leakage effects, considering a limited range of Stokes coefficients. The final error is ~25 mm, demonstrating the ability of GRACE to improve knowledge of the water cycle over the HPA and to recover groundwater storage variations using appropriate methods.

[53] With suitable concentration and filter methods, it is possible to divide the HPA into two subregions, demonstrating that GRACE can be used effectively with basins as small as ~200,000 km<sup>2</sup>, with irregular shapes. The shorter 10-day temporal sampling of GRGS solution also appears to provide useful monitoring of rapid water storage variations, such as those related to groundwater pumping.

[54] An important lesson from this study is dependence on oceanic and atmospheric models, as well as data-assimilating land surface models such as GLDAS to optimize the use of GRACE data. While a goal of the GRACE mission is to provide independent measures of the water cycle, it is clear,

especially for smaller basins, that an iterative analysis will be most effective. In all future gravity measurements from space, it is anticipated that land surface models will continue to guide the formulation of GRACE water storage variation estimates as, in turn, GRACE or other gravity satellite estimates contribute to land surface models.

[55] **Acknowledgments.** Funding for this study was provided by National Aeronautics and Space Administration grant NNX08AJ84G and the Jackson School of Geosciences at the University of Texas at Austin. We are grateful to H. Rajaram and T. Illangasekare as well as the three anonymous reviewers who helped in improving the paper. We thank M. Dunklee from the U.S. Geological Survey-SCAN (Soil Climate Analysis Network); W. Burgett from the West Texas Mesonet; J. Basara from the Oklahoma Mesonet; N. Umphlett from the High Plains Regional Climate Center, the Atmospheric Radiation Measurement Program; and D. Wedin for making available soil moisture measurements for this study. We thank F. Simon for fruitful discussion on spatio-spectral localization. His computer algorithms are available on [www.fredrik.net](http://www.fredrik.net). Computational resources were provided by E. Jarrett of the Department of Geological Sciences, University of Texas at Austin. We thank G. Strassberg for his assistance and advice.

## References

- Baur, O., M. Kuhn, and W. E. Featherstone (2009), GRACE-derived ice-mass variations over Greenland by accounting for leakage effects, *J. Geophys. Res.*, *114*, B06407, doi:10.1029/2008JB006239.
- Bettadpur, S. (2007), *Level-2 Gravity Field Product User Handbook*, GRACE 327-734, The GRACE Project, Center for Space Research, University of Texas, Austin, TX, USA.
- Chambers, D. P. (2006), Evaluation of new GRACE time-variable gravity data over the ocean, *Geophys. Res. Lett.*, *33*(17), L17603, doi:10.1029/2006GL027296.
- Chen, J. L., C. R. Wilson, J. S. Famiglietti, and M. Rodell (2005), Spatial sensitivity of the Gravity Recovery and Climate Experiment (GRACE) time-variable gravity observations, *J. Geophys. Res.*, *110*, B08408, doi:10.1029/2004JB003536.
- Chen, J. L., C. R. Wilson, J. S. Famiglietti, and M. Rodell (2007), Attenuation effect on seasonal basin-scale water storage change from GRACE time-variable gravity, *J. Geodesy*, *81*, 237–245.
- Chen, J. L., C. R. Wilson, B. D. Tapley, Z. L. Yang, and G. Y. Niu (2009), 2005 drought event in the Amazon River basin as measured by GRACE and estimated by climate models, *J. Geophys. Res.*, *114*, B05404, doi:10.1029/2008JB006056.
- Dahlen, F. A., and F. J. Simons (2008), Spectral estimation on a sphere in geophysics and cosmology, *Geophys. J. Int.*, *174*, 774–807, doi:10.1111/j.1365-246X.2008.03854.x.
- Daly, C., M. Halbleib, J. I. Smith, W. P. Gibson, M. K. Doggett, G. H. Taylor, J. Curtis, and P. A. Pasteris (2008), Physiographically sensitive mapping of climatological temperature and precipitation across the conterminous United States, *Int. J. Climatol.*, *28*(15), 2031–2064, doi:10.1002/joc.1688.
- Dickey, J. O., and the National Research Council Committee on Earth Gravity from Space (1997), *Satellite Gravity and the Geosphere: Contributions to the Study of the Solid Earth and Its Fluid Envelope*, National Academy Press, Washington, D. C.
- DiLuzio, M., G. L. Johnson, C. Daly, J. K. Eischeid, and J. G. Arnold (2008), Constructing retrospective gridded daily precipitation and temperature datasets for the conterminous United States, *J. Appl. Meteorol. Climatol.*, *47*, 475–497.
- Dziewonski, A., and D. Anderson (1981), Preliminary reference earth model, *Phys. Earth Planet Int.*, *25*, 297–356.
- Fenoglio-Marc, L., J. Kusche, and M. Becker (2006), Mass variation in the Mediterranean Sea from GRACE and its validation by altimetry, steric and hydrology fields, *Geophys. Res. Lett.*, *33*, L19606, doi:10.1029/2006GL026851.
- Güntner, A. (2008), Improvement of global hydrological models using GRACE data, *Surv. Geophys.*, *29*, 375–397, doi:10.1007/s10712-008-9038-y.
- Guo, J., Y. Li, H. Deng, S. Xu, and J. Ning (2004), Green's function of the deformation of the earth as a result of atmospheric loading, *Geophys. J. Int.*, *159*, 53–68.
- Guo, J. Y., X. J. Duan, C. K. Shum (2010), Non-isotropic Gaussian smoothing and leakage reduction for determining mass changes over

- land and ocean using GRACE data, *Geophys. J. Int.*, *181*(1), 290–302, doi:10.1111/j.1365-246X.2010.04534.x.
- Han, S. C., C. K. Shum, C. Jekeli, C. Y. Kuo, C. R. Wilson, and K. W. Seo (2005), Non-isotropic filtering of GRACE temporal gravity for geophysical signal enhancement, *Geophys. J. Int.*, *163*, 18–25, doi:10.1111/j.1365-246X.2005.02756.x.
- Han, S.-C., and F. J. Simons (2008), Spatiospectral localization of global geopotential fields from the Gravity Recovery and Climate Experiment (GRACE) reveals the coseismic gravity change owing to the 2004 Sumatra-Andaman earthquake, *J. Geophys. Res.*, *113*, B01405, doi:10.1029/2007JB004927.
- Han, S.-C., H. Kim, I. Y. Yeo, P. Yeh, T. Oki, K.-W. Seo, D. Alsdorf, and S. B. Luthcke (2009), Dynamics of surface water storage in the Amazon inferred from measurements of inter-satellite distance change, *Geophys. Res. Lett.*, *36*, L09403, doi:10.1029/2009GL037910.
- Jekeli, C. (1981), Alternative methods to smooth the Earth's gravity field. *Rep. 327*, Dept. of Geod. and Sci. and Surv., Ohio State Univ., Columbus, OH, USA.
- Klees, R., E. A. Zapreeva, H. C. Winsemius, and H. H. G. Savenije (2007), The bias in GRACE estimates of continental water storage, *Var. Hydrol. Earth Syst. Sci.*, *11*, 1227–1241.
- Klees, R., E. A. Revtova, B. C. Gunter, P. Ditmar, E. Oudman, H. C. Winsemius and H. H. G. Savenije (2008a), The design of an optimal filter for monthly GRACE gravity models, *Geophys. J. Int.*, *175*, 417–432.
- Klees, R., X. Liu, T. Wittwer, B. C. Gunter, E. A. Revtova, R. Tenzer, P. Ditmar, H. C. Winsemius, and H. H. G. Savenije (2008b), A Comparison of Global and Regional GRACE Models for Land Hydrology, *Surv. Geophys.*, *29*(4–5), 335–359, doi:10.1007/s10712-008-9049-8.
- Kusche, J. (2007), Approximate decorrelation and non-isotropic smoothing of time-variable GRACE-type gravity field models, *J. Geod.*, *81*, 733–749.
- Leblanc, M. J., P. Tregoning, G. Ramillien, S. O. Tweed, and A. Fakes (2009), Basin-scale, integrated observations of the early 21st century multiyear drought in southeast Australia, *Water Resour. Res.*, *45*, W04408, doi:10.1029/2008WR007333.
- Lemoine, J.-M., S. Bruinsma, S. Loyer, R. Biancale, J.-C. Marty, F. Perosanz, and G. Balmino (2007), Temporal gravity field models inferred from GRACE data, *Adv. Space Res.*, *39*, 1620–1629, doi:10.1016/j.asr.2007.03.062.
- Lettenmaier, D. P., and J. S. Famiglietti (2006), Hydrology: water from on high, *Nature*, *444*(7119), 562–563.
- Longuevergne, L., N. Florsch, and P. Elsass (2007), Extracting coherent regional information from local measurements with Karhunen-Loève transform: Case study of an alluvial aquifer (Rhine valley, France and Germany), *Water Resour. Res.*, *43*, W04430, doi:10.1029/2006WR005000.
- McGuire, V. L. (2007), Water-level changes in the High Plains aquifer, predevelopment 482 to 2005 and 2003 to 2005, *U.S. Geological Survey Scientific Investigation Report 483 2006-5324*, 7 pp.
- Ngo-Duc, T., K. Laval, G. Ramillien, J. Polcher, and A. Cazenave (2007), Validation of the land water storage simulated by organising carbon and hydrology in dynamic ecosystems (ORCHIDEE) with gravity recovery and climate experiment (GRACE) data, *Water Resour. Res.*, *43*, W04427, doi:10.1029/2006WR004941.
- Niu, G.-Y., and Z.-L. Yang (2006), Assessing a land surface model's improvements with GRACE estimates, *Geophys. Res. Lett.*, *33*, L07401, doi:10.1029/2005GL025555.
- Pagiatakis, S. (1990), The response of a realistic Earth to ocean tide loading, *Geophys. J. Int.*, *103*, 541–560.
- Percival, D. B., and A. T. Walden (1993), *Spectral Analysis for Physical Applications, Multitaper and Conventional Univariate Techniques*, Cambridge Univ. Press, New York.
- Ramillien, G., F. Frappart, A. Cazenave, and A. Güntner (2005), Time variations of land water storage from an inversion of 2 years of GRACE geoids, *Earth Planet Sci. Lett.*, *235*(1–2), 283–301.
- Ramillien, G., F. Frappart, A. Güntner, T. Ngo-Duc, and A. Cazenave (2006), Mapping time variations of evapotranspiration rate from GRACE satellite gravimetry, *Water Resour. Res.*, *42*, W10403, doi:10.1029/2005WR004331.
- Ramillien, G., J. S. Famiglietti, and J. Wahr (2008), Detection of continental hydrology and glaciology signals from GRACE: a review, *Surv. Geophys.*, *29*, 361–374, doi:10.1007/s10712-008-9048-9.
- Rodell, M., and J. S. Famiglietti (2002), The potential for satellite-based monitoring of groundwater storage changes using GRACE: the High Plains aquifer, Central US, *J. Hydrol.*, *263*(1–4), 245–256.
- Rodell, M., et al. (2004a), The global land data assimilation system, *Bull. Am. Meteorol. Soc.*, *85*(3), 381–394.
- Rodell, M., J. S. Famiglietti, J. Chen, S. I. Seneviratne, P. Viterbo, S. Holl, and C. R. Wilson (2004b), Basin scale estimates of evapotranspiration using GRACE and other observation, *Geophys. Res. Lett.*, *31*, L20504, doi:10.1029/2004GL020873.
- Rodell, M., I. Velicogna, and J. S. Famiglietti (2009), Satellite-based estimates of groundwater depletion in India, *Nature*, *460*, 999–1002, doi:10.1038/nature08238.
- Rowlands, D. D., S. B. Luthcke, S. M. Klosko, F. G. Lemoine, D. S. Chinn, J. J. McCarthy, C. M. Cox, and O. B. Anderson (2005), Resolving mass flux at high spatial and temporal resolution using GRACE intersatellite measurements, *Geophys. Res. Lett.*, *32*, L04310, doi:10.1029/2004GL021908.
- Sasgen, I., Z. Martinec, and K. Fleming (2006), Wiener optimal filtering of GRACE data, *Stud. Geophys. Geod.*, *50*, 499–508.
- Save, H. V. (2009), Using regularization for error reduction in GRACE gravity estimation, PhD dissertation, University of Texas at Austin, 113 pp.
- Schmidt, R., F. Flechtner, U. Meyer, K. H. Neumayer, C. Dahle, R. König, and J. Kusche (2008), Hydrologic signals observed by the GRACE satellites, *Surv. Geophys.*, *29*(4–5), 319–334, doi:10.1007/s10712-008-9033-3.
- Simons, F. J., and A. Dahlen (2008), Spherical Slepian functions and the polar gap in geodesy, *Geophys. J. Int.*, *166*, 1039–1061.
- Simons, F. J., F. A. Dahlen, and M. A. Wieczorek (2006), Spatiospectral concentration on a sphere, *SIAM Rev.*, *48*, 504–536, doi:10.1137/S0036144504445765.
- Seo, K. W., and C. R. Wilson (2005), Simulated estimation of hydrologic loads from GRACE, *J. Geod.*, *78*, 442–456.
- Seo, K.-W., C. R. Wilson, J. S. Famiglietti, J. L. Chen, and M. Rodell (2006), Terrestrial water mass load changes from gravity recovery and climate experiment (GRACE), *Water Resour. Res.*, *42*, W05417, doi:10.1029/2005WR004255.
- Seo, K.-W., C. R. Wilson, J. Chen, and D. E. Waliser (2008), GRACE's spatial aliasing error, *Geophys. J. Int.*, *172*, 41–48, doi:10.1111/j.1365-246X.2007.03611.x.
- Slepian, D. (1978), Prolate spheroidal wave functions, Fourier analysis, and uncertainty V: The discrete case, *Bell Syst. Tech. J.*, *57*, 1371–430.
- Strassberg, G., B. R. Scanlon, and M. Rodell (2007), Comparison of seasonal terrestrial water storage variations from GRACE with groundwater-level measurements from the High Plains Aquifer (USA), *Geophys. Res. Lett.*, *34*, L14402, doi:10.1029/2007GL030139.
- Strassberg, G., B. R. Scanlon, and D. Chambers (2009), Evaluation of Groundwater Storage Monitoring with the GRACE Satellite: Case Study High Plains Aquifer, Central USA, *Water Resour. Res.*, *45*, W05410, doi:10.1029/2008WR006892.
- Swenson, S., and J. Wahr (2002), Methods for inferring regional surface-mass anomalies from GRACE measurements of time-variable gravity, *J. Geophys. Res.*, *107*(B9), 2193, doi:10.1029/2001JB000576.
- Swenson, S., and J. Wahr (2006), Post-processing removal of correlated errors in GRACE data, *Geophys. Res. Lett.*, *33*, L08402, doi:10.1029/2005GL025285.
- Swenson, S., and J. Wahr (2007), Multi-sensor analysis of water storage variations of the Caspian Sea, *Geophys. Res. Lett.*, *34*, L16401, doi:10.1029/2007GL030733.
- Swenson, S., J. Wahr, and P. C. D. Milly (2003), Estimated accuracies of regional water storage variations inferred from the Gravity Recovery and Climate Experiment (GRACE), *Water Resour. Res.*, *39*(8), 1223, doi:10.1029/2002WR001808.
- Syed, T. H., J. S. Famiglietti, M. Rodell, J. Chen, and C. R. Wilson (2008), Analysis of terrestrial water storage changes from GRACE and GLDAS, *Water Resour. Res.*, *44*, W02433, doi:10.1029/2006WR005779.
- Syed, T. H., J. S. Famiglietti, D. Chambers (2009), GRACE-based estimates of terrestrial freshwater discharge from basin to continental scales, *J. Hydrometeorol.*, *10*(1), 22–40, doi:10.1175/2008JHM993.1.
- Tapley, B. D., S. Bettadpur, J. C. Ries, P. F. Thompson, and M. M. Watkins (2004), GRACE measurements of mass variability in the Earth system, *Science*, *305*(5683), 593–505, doi:10.1126/science.1099192.
- Thomson, D. J. (1982), Spectrum estimation and harmonic analysis, *Proc. IEEE*, *70*, 1055–1096.
- Tiwari, V. M., J. Wahr, and S. Swenson (2009), Dwindling groundwater resources in northern India from satellite gravity observations, *Geophys. Res. Lett.*, *36*, L18401, doi:10.1029/2009GL039401.
- Velicogna, I., and J. Wahr (2006), Measurements of time-variable gravity show mass loss in Antarctica, *Science*, *311*, 1754–1756.

- Wahr, J., M. Molenaar, and F. Bryan (1998), Time variability of the earth's gravity field: Hydrologic and oceanic effects and their possible detection using GRACE, *J. Geophys. Res.*, *103*, 30,205– 30,230, 1998.
- Wahr, J., S. Swenson, V. Zlotnicki, and I. Velicogna (2004), Time-variable gravity from GRACE: First results, *Geophys. Res. Lett.*, *31*, L11501, doi:10.1029/2004GL019779.
- Wahr, J., S. Swenson, and I. Velicogna (2006), Accuracy of GRACE mass estimates. *Geophys. Res. Lett.*, *33*(6), L06401, doi:10.1029/2005GL025305.
- Werth, S., A. Güntner, S. Petrovic, and R. Schmidt (2009), Integration of GRACE mass variations into a global hydrologic model, *Earth Planet. Res. Lett.*, *277*(1–2), 166–173.
- Wicczorek, M. A., and F. J. Simons (2005), Localized spectral analysis on the sphere, *Geophys. J. Int.*, *162*, 655–675, doi:10.1111/j.1365-246X.2005.02687.x.
- Zaitchik, B. F., M. Rodell, and R. H. Reichle (2008), Assimilation of GRACE terrestrial water storage data into a land surface model: results for the Mississippi river basin. *J. Hydrometeorol.*, *9*, 535–548.
- 
- L. Longuevergne and B. R. Scanlon, Bureau of Economic Geology, Jackson School of Geosciences, University of Texas at Austin, 10100 Burnet Rd., Austin, TX 78758, USA. (laurent.longuevergne@beg.utexas.edu)  
C. R. Wilson, Department of Geological Sciences, Jackson School of Geosciences, University of Texas at Austin, 1 University Station C1100, Austin, TX 78712, USA.